DIFFRACTION OF THE SINGULAR BEAM ON AN OPAQUE SCREEN AND REGENERATION OF AN OPTICAL VORTEX

V.N. GORSHKOV, A.N. KHOROSHUN[1], M.S. SOSKIN

Institute of Physics, Nat. Acad. Sci. of Ukraine
(46, Nauky Prosp., Kyiv 03650, Ukraine),

[1]**East Ukrainian National University**
(20a, Molodezhny block, Lugansk 91034, Ukraine)

UDC 535.2

We have developed the theory of diffraction of the singular light beam with axial optical vortex on a half-plane screen which cuts off the vortex zero-amplitude center ("severe screening"). It is shown that such diffraction features differ strongly from the well-known diffraction of a light beam with smooth wave front. It is found that the singular properties of the beam are restored at some distance behind the screen due to the influence of long-wave transversal perturbations. This is happened through the complicated space dynamics due to the generation of secondary short-living "diffractive" vortices. The diffraction is considered for one and many charged singular beams. We have established the duration, possibility, and quality of the regeneration of the helicoidal structure of the wave front basing on the developed mathematical model and the analysis of the distributions of amplitude, phase, and orbital angular momentum (OAM).

1. Introduction

The unique properties [1] of optical vortices (OVs) are actively investigated in modern optics [2—5]. They are determined by the zero value of the complex amplitude on the OV beam axis, and hence the phase is undefined. As a result, the wave front acquires the shape of a helicoid, causing the precession of the Poynting vector. A phase change after the circumvention of the zero-amplitude axis equals $2m\pi$, where the number m defines its topological charge. Surprising fundamental properties of a vortex provide its ability to catch particles due to the different pressures of light at the center and at the edge of an optical trap and to rotate them [6]. This phenomenon opens prospects for the development of optical tweezers, multichannel manipulators of microparticles, optical processors, devices of sorting according to the sizes of similar objects, whose sizes are less than the used radiation wavelength.

The extensive application of optical vortices causes the actuality of researches of mechanisms of their formation and delimitation of practical use [7, 8]. We will concentrate in this paper on a computer modelling of most interesting cases of the restoring of a singular beam. We qualify the investigated case as "severe screening" because more than half the beam cross-section is blocked, i.e. the zero-amplitude "heart" of the optical vortex is cut. This screening kills the vortex because the points with fully destructive interference are absent just after the screen. Therefore, the regeneration of such a severely screened vortex beam is not obvious from the very beginning and can occur through the generation of secondary vortices only. The answer to this question is the main task of our theory.

On the whole, for $|m|$ greater than 1, the beam is not steady and breaks up into m one-charge vortices. Moreover, for beams with $m = -3$ and $m = -5$, one observes the regeneration of the helicoidal structure of their wave fronts at some distance from the obstacle as the appearance of, respectively, three and five vortices.

This surprising property of a singular beam is revealed at studying the evolution of the vortex beam diffraction by means of the analysis of the distributions of the amplitude, phase, and OAM. The OAM is caused by different azimuth components of the Umov—Poynting vector for different angles and contains the

memory about the initial helical wave front. We have investigated the dynamics of vortex beam diffraction and the possibility and quality of its regeneration. Such analysis is actual both for the fundamentals of singular optics and for the application of singular beams to the information transmission and processing.

2. Mathematical Model

Our main task is to study the spatial dynamics of a severely screened vortex beam and to describe the mechanisms of topological reactions causing the regeneration. By reducing the three-dimensional space problem to a two-dimensional "dynamical" problem on the plane XY, we have developed the mathematical description and qualitative analysis of the evolution of a diffractive beam along the Z-axis which plays the role of time τ in such an approach.

Let us consider a linearly polarized light beam propagating along the Z-axis. The vector potential of this light field equals $\hat{A} = nU(x,y,z)$, where n is the unit vector for a given polarization. Then the magnetic induction $B = \mathrm{rot}A$, and electric field intensity equals

$$E = -\frac{1}{c}\frac{\partial A}{\partial t}.$$

A general solution of the wave equation $\frac{1}{c^2}\frac{\partial^2 U}{\partial t^2} = \Delta U$ for the z-propagation of the beam in the paraxial approximation is the function

$$U(x,y,z) = U_0(x,y,z)\cos[\omega t - kz \mp \Phi(x,y,z)] =$$

$$= [u + iv]\exp[i(wt - kz)],$$

$$U_0 = \sqrt{u^2 + v^2}, \quad \Phi = \mathrm{Arc}\tan\left(\frac{v}{u}\right),$$

$$u = U_0\cos\Phi, \quad v = U_0\sin\Phi.$$

In the paraxial approximation, the complex amplitude $A = u + iv$ satisfies the Leontovich parabolic equation

$$\frac{\partial A}{\partial z} = \frac{1}{2ik}\Delta A, \tag{1}$$

where Δ is the Laplace operator in the XY plane.

Equation (1) under the formal replacement of z by the conditional time τ transforms to the Schrödinger equation which describes the dynamics of a light beam on the XY plane. It represents the expansion of the beam as a diffusion process of some initial distribution of the light field at the moment $\tau = \tau_0 \equiv 0$. Since the "coefficient of diffusion" $\frac{1}{2ik}$ in Eq. (1) is imaginary, the diffusion of the amplitude is accompanied by a change of the phase. The beam expansion has the wave character for the "components" u and v of the field which satisfy the system of equations

$$\frac{\partial u}{\partial \tau} = \frac{1}{4}\left(\frac{\partial^2 v}{\partial x^2} + \frac{\partial^2 v}{\partial y^2}\right), \quad \frac{\partial v}{\partial \tau} = -\frac{1}{4}\left(\frac{\partial^2 u}{\partial x^2} + \frac{\partial^2 u}{\partial y^2}\right). \tag{2}$$

We use the dimensionless variables $\tau \Rightarrow z/L_{\mathrm{R}}$, $x, y \Rightarrow x/r_0, y/r_0$, where r_0 is the beam waist radius and $L_{\mathrm{R}}/2$ is the Rayleigh length. System (2) for the disturbance as plane waves

$$u = u_0\exp[i(\hat{\omega}\tau - \mathbf{kr})], \mathrm{v} = \mathrm{v}_0\exp[\mathrm{i}(\hat{\omega}\tau - \mathbf{kr})] \tag{3}$$

leads to the dispersion relation in the simplest one-dimensional case

$$\hat{\omega} = \frac{1}{4}k_{\perp}^2. \tag{4}$$

This corresponds to the wavelength-dependent phase velocity

$$\hat{v}_{\mathrm{ph}} = \frac{\hat{\omega}}{k_{\perp}} = \frac{k_{\perp}}{4}. \tag{5}$$

The parameter $k_{\perp}$ defines the period of oscillations of the u and v functions in the plane. Expressions (3) and (4) yield the relation $u_0 = iv_0$. Therefore, the waves of the v-components are delayed by the $\pi/2$ phase relative to the u-components, i.e. they are shifted by a quarter of the wavelength.

The amplitude A of an undisturbed singular beam with axial optical vortex can be written in a self-similar way in the cylindrical coordinates as

$$A(\rho,\varphi,\tau) = \frac{A_0}{\sqrt{1+\tau^2}}\left(\frac{\rho}{\sqrt{1+\tau^2}}\right)^m \times$$

$$\times \exp\left(\frac{\rho^2}{1+\tau^2}\right)\exp(i\Phi(\rho,\varphi,\tau)),$$

$$\Phi(\rho,\varphi,\tau) = (|m+1|)\mathrm{arctan}\tau - \frac{\rho^2\tau}{1+\tau^2} + m\varphi.$$

Here, the dimensionless variable $\rho = \sqrt{x^2+y^2}/r_0$, and m is the topological charge of a vortex.

On the one hand, relations (4) and (5) have completely transparent physical sense and, on the other hand, can be the basis in the analysis of various mechanisms of formation of vortices in a disturbed beam. The screen forms the distribution of perturbed streams on the XY plane with the expressed heterogeneity of a characteristic wave vector $\mathbf{k}$ (the propagation speed

of field perturbations). The development of such a heterogeneity in time τ results in a radical reconstruction of the wave front of the beam, which corresponds to the appearance of the destructive interference.

At first, we determine the physical sense of the parameters $\hat{\omega}$ and k.

Any beam can be expanded into plane waves, $\exp(i\omega\tau - ik_{\mathbf{p}}z - i\mathbf{k}_{\perp}\mathbf{r})$, which expand at different angles to the axis Z: $|\mathbf{k}| = |\mathbf{k_p} + \mathbf{k}_{\perp}| = \text{const} = 2\pi/\lambda$. In the phase of this plane wave, we neglect its fast oscillating component $(i\omega t - ikz)$ and operate with the "slow" component Φ. Then

$$\Phi = [(k - k_{\mathbf{p}})z - \mathbf{k}_{\perp}\mathbf{r}] \approx \frac{k_{\perp}^2}{2k}z - \mathbf{k}_{\perp}\mathbf{r} \tag{6}$$

as $\frac{k_{\perp}}{k} = 1$.

Due to the use of the dimensionless variable in (6) as in (2), we get the known equality

$$\Phi = \hat{\omega}\tau - \mathbf{kr}, \quad \hat{\omega} = \frac{\mathrm{k}^2}{4}, \quad \mathbf{k} = \mathbf{k}_{\perp}\mathrm{r}_0. \tag{7}$$

The distance between the equal-phase lines is (in the real sizes) $\lambda_{\perp} = {}^{2\pi}/_{k_{\perp}}$. They move with speed (5) on the XY plane in the course of time τ. The change of Φ along the Z-axis is much weaker.

Thus, on the base of Eqs. (2), we investigate the temporal evolution of the "projection" of the light field varying in space on the XY plane. For the general signal of plane waves, the dynamics of the slow phase Φ is described by Eqs. (4), (5), and (7).

We emphasize a very important role of the "slow" phase $\Phi(x, y, z(\tau))$ in studying the evolution of a beam during its propagation. The form of the wave surface of the beam is defined by the equation

$$-kz + \Phi(x, y, z(\tau)) = \text{const}. \tag{8}$$

We are interested in the form of the wave front in the high-intensity field of the beam where the value of z changes within the scope of several wavelengths. In this case, it is possible to neglect a change of the slow phase in relation (8), and then it is equal to $\Phi(x, y, z_0(\tau_0))$, where z_0 is the distance from the obstacle. Then the equation of a wave surface in the area of interest $z \approx z_0$ is

$$z = \Phi(x, y, \tau_0)/k, \tag{9}$$

where τ_0 is the "evolution time" of the beam on a distance z.

Let's consider topological reactions between separate sheets of the wave surface of the regeneration of optical vortices.

Surface (9) in the perturbed beam has complex form. The appearance of destructive interference at the point $M(x_0, y_0, z_0)$ has the prehistory in the transformation of the wave front of the light field in a vicinity of a straight line $(x = x_0, y = y_0)$. This transformation leads to a growing difference of $k_{\perp}$ between two neighbour perturbations. As a result, a phase ledge appears on the wavefront. When the height of this ledge reaches the critical $\lambda/2$ value, the signals come to the point $M(x_0, y_0, z_0)$ "from the right" and "from the left" with the π difference of the phases. At this moment, both the destructive interference and the vortical structure of the light field appear.

3. Nucleation of Short-living "Diffractive" Vortices in the Transparent Part of a Screened Vortex Beam

The developed approach describes naturally the widening and the self-similar propagation of an undisturbed singular beam through the excitation of transverse waves. Their wavelengths are of the order of the waist radius r_0 for small τ, and the amplitudes are defined by the second derivatives of the initial distribution of components and are proportional to $1/r_0^2$. The same model is effective for the investigation of the diffraction dynamics of screened singular beams. Short-wavelength waves appear near the screen edge at small τ and propagate with high phase velocity perpendicularly to it in both directions. The a-type waves are symmetric relative to the Y-axis with a relatively smooth phase distribution. In contrary, b-type waves are antisymmetric and possess the π-jump on the line $x = 0$. It is known [13] that two conditions have to be fulfilled simultaneously at the points of vortex nucleation: (i) equality of competing amplitudes $|A_a| = |A_b|$ and (ii) π-shift of their phases. These conditions can be realized in the zones of relatively smooth phase variations of a-waves (Fig. 1,*a*) and drastic phase variations of b-waves (Fig. 1,*b*). As a result, the final phase map of the diffracted beam $\Phi(x, y, 0.5)$ (Fig. 1,*c*) contains a nearly vertical fold in the central part. It is accompanied by lines 1 of the equality of the partial amplitudes A_a and A_b. And only one point exists on each line, where the single-charged secondary vortices are born. They possess opposite charges according to the law of topological charge conservation [15, 16].

The dipole of vortices (Fig. 1,*c*) is located in the *transparent* part of the beam cross-section *behind* the main intensity "mountain" and is oriented along equiphase lines. As we see, the residual helical wave-

front structure didn't play a significant role in these events. Due to this fact, it is no surprise that the phase spiral is not restored still. It is the base to mark these firstly appeared secondary vortices in the transparent part as "diffractive" vortices. The left vortex in the dipole is located on the left slope of the $A_b(x \approx 0, y, \tau)$, where the energy flow is something higher on the left side. Due to this, the general energy circulation is clockwise and opposite to the phase growth direction. The opposite situation is realized for the right vortex. Therefore, the vector of orientation of dipoles of diffracted vortices doesn't depend on the sign of the topological charge of the initial vortex.

All diffractive vortices annihilate rapidly at $\tau \geq 1$ due to the "cleaning" of the diffracted beam from short-wavelength transverse waves and don't play any significant role in the "self-restoration" of a screened singular beam. The next act of the real self-treatment of a severely screened vortex beam is started in the diffracted beam shadow part after the "long" time, and the remained vorticity plays a decisive role in this process.

4. Stable "Regenerated Vortices" and Dynamics of Vortex Beam "Self-Treatment"

The first dipole of secondary vortices in the beam shadow part nucleates at $\tau = 0.9$ just in the intensity ravine. Therefore, it is oriented across equiphase lines in contrary to the dipoles of diffractive vortices (Fig. 2,*a*). When "time" grows, the vortex with the "native" sign survives during the space dynamics of a diffracted beam, but the vortex with opposite sign moves to the periphery and disappears to $\tau = 3$ (Fig.2,*b*). This is the reason to call stable vortices in the shadow part with initial sign as *regenerated* vortices. It is important that, to this moment, the phase spiral with the initial direction of rotation is restored. This gives a good reason to conclude that namely the restoration of a helix wave-front structure leads to the nucleation of regenerated vortices.

The vortex beam amplitude structure at $\tau = 3$ after the regeneration is presented in Fig. 3. The hole of the regenerated vortex is clearly seen. It is remarkable that the strong amplitude tail is extended in parallel to the screen edge. The comparison of this asymmetric structure with axial symmetric crater-like structure of the incident beam at $\tau = 3$ shows how strongly they differ. It is evident that the "self-restored" beam loses the self-similarity during the propagation inherent to axial

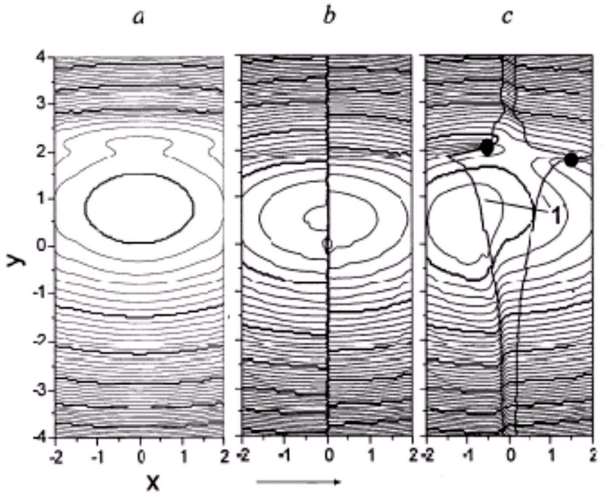

Fig. 1. Phase maps of a screened vortex beam ($m = -1$, $y_s = 0.1$, $\tau = 0.5$): a — $\Phi_a(x, y, 0.5)$ b — $\Phi - B(x, y, 0.5)$, c — $\Phi - C(x, y, 0.5)$; l — lines where $\mid A_a(x, y, 0.5) \mid = \mid A_b(x, y, 0.5) \mid$. Filled circles form the dipole of born diffractive vortices

vortex beams. But nevertheless, it is again a *singular* beam.

To better understand the inner mechanism of the regeneration of a diffracted vortex beam, we have to take into account the action of the residual helical structure and OAM on the diffracted beam dynamics. To do this, we have found them for a "long" time, ($\tau = 3$), of the evolution (Fig. 4). The equiphase and equiamplitude lines are presented together with the space distribution of the OAM density $M_z(x, y)$. The shadow domain is the location of OAM with the initial sign of the vortex, and the clean domain possesses the opposite sign of $M_z(x, y)$. We see again the limited annihilation of diffractive vortices and the regeneration of the vortex near the beam axis. Most interesting is the redistribution of the amplitude and, especially, OAM, which is defined by the azimuth component of the Poynting vector. It is seen that the amplitude maximum don't coincide with the phase maximum. The Poynting vector is inclined to the right. Therefore, it is natural that the amplitude maximum was rotated clockwise from the initial position on the y-axis above the screen edge nearly by $\pi/2$. It is remarkable that this rotation takes place in the opposite direction to the counterclockwise rotation of the phase helicoid.

Much more complicated and interesting is the OAM density distribution in the central part of a diffracted vortex beam. The domain with the initial sign of M_z contains the island of M_z with opposite sign. It is clear that the center of each appeared vortex has to be located

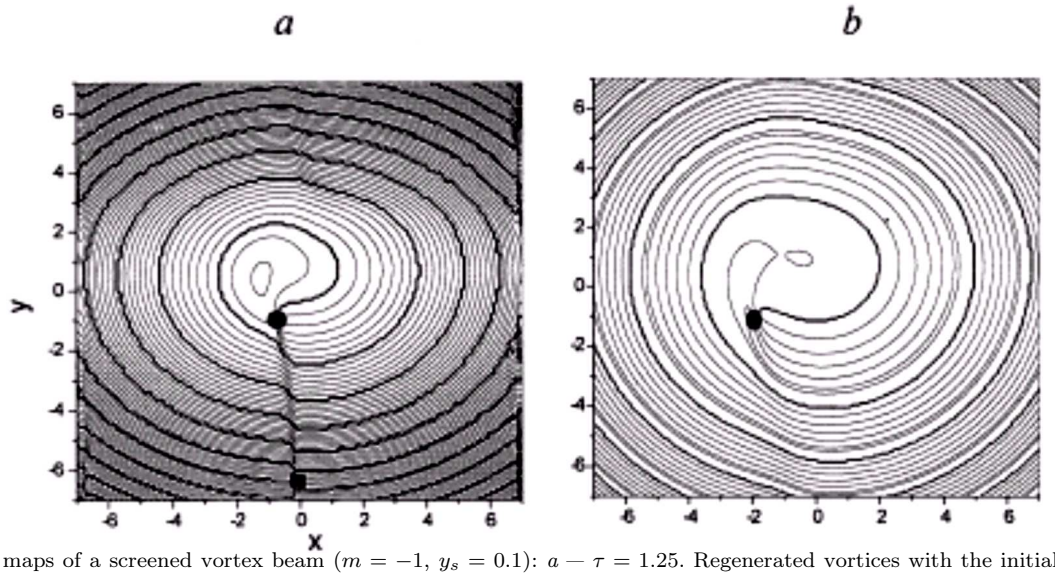

Fig. 2. Phase maps of a screened vortex beam ($m = -1$, $y_s = 0.1$): a — $\tau = 1.25$. Regenerated vortices with the initial (filled circle) and opposite (filled square) signs are seen, b — $\tau = 3$ (one regenerated vortex with the initial sign remains)

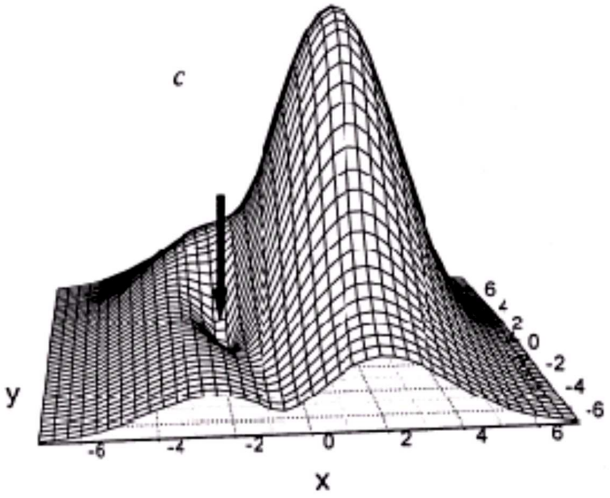

Fig.3. Amplitude distribution $| A(x, y, 3) |$ (black arrow shows the location of a born regenerated vortex)

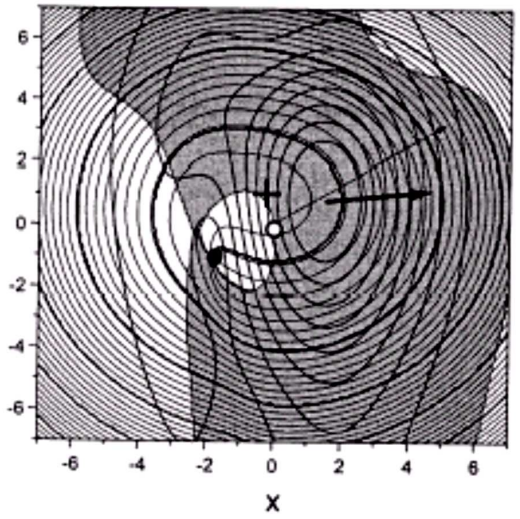

Fig. 4. Phase map (equiphase spiral lines), amplitude distribution (closed lines), and orbital angular momentum density distributions (shadow and white domains) for a self-restored vortex beam at $\tau = 3$ are presented: the shadow circle is the position of a the beam axis, filled circle is the position of regenerated vortex, thin arrow is the radius-vector from the beam axis to the location of the amplitude maximum, thick arrow is the direction of the Poynting vector at the point of the amplitude maximum

on the zero-line $M_z = 0$, because $M_z = 0$ at the vortex center due to its zero-amplitude value [17]. Indeed, the regenerated vortex is located on the border line between domains with positive and negative values of M_z, where M_z =0. The difference of energy flows from the left and right parts of the screened beam together with the existence of a vertical line with the π difference near it (Fig. 1,c) define the nucleation dipoles of regenerated vortices in the beam shadow part out of the zone of maximal amplitudes of the diffracted beam and their orientation across equiphase lines. The developed model allows us to evaluate the duration of the vortex beam self-restoration by using the system of equations

$$\begin{cases} y_{VR} \approx \sqrt{1+\tau_R^2} & (*) \\ \tau_R \approx y_{VR}/\nu_{\rm ph} & (**) \end{cases} .$$

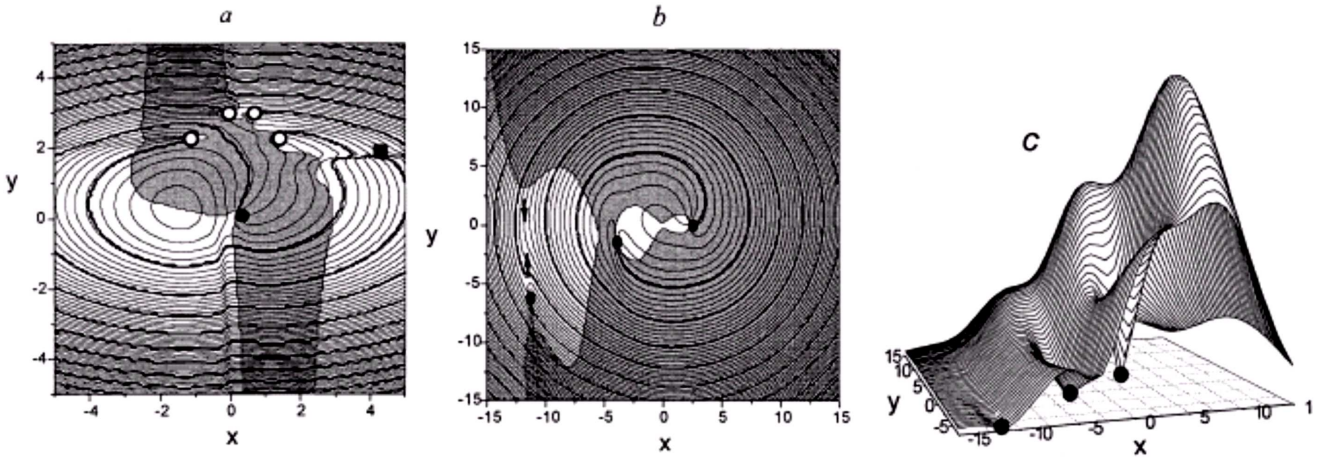

Fig. 5. Phase map (equiphase lines) and orbital angular momentum density distributions (shadow and white domains) of a diffracted three-order vortex at $\tau = 0.5$ (a). Phase map at $\tau = 7$ (b) and the amplitude distribution $\mid A(x, y, 7) \mid$ at $m = 3$ (c)

The first equation describes the expansion of an undisturbed beam and the second one does the displacement of a vortex structure along the Y-axis. This gives two times: $\tau_1 \approx 0.5$ for the beginning and $\tau_2 \approx 2$ as the fulfilment of the screened beam self-treatment. The obtained values coincide well enough with those obtained by the direct modelling. In the general case, the regeneration time for a singular beam (the distance z behind a screen) is defined by the residual helicity at $\tau = 0$ ($z = 0$). It can be evaluated as the ratio of the total OAM (calculated to the "mass center") to the integral intensity, if we will consider the light intensity as the surface "mass density". This parameter is connected with the difference of the clock- and counterclockwise energy flows on the screen edge on the right and on the left from the Y-axis, which plays a decisive role in the singular beam self-treatment.

So, the screened vortex beam diffraction dynamics clearly differs at "short" and "long" distances. The usual diffraction plays a dominant role, and the phase helicoid is still not restored at short distances. In contrary, all diffractive vortices annihilate, the phase spiral is restored, and the vortex with initial sign is regenerated due to the influence of long-wave transversal perturbations at long distances.

5. Self-Restoration of a Higher-Order Vortex Beam

To check the validity of these conclusions for higher-order vortices, the self-restoration of a severely screened beam with axial higher-order vortex was considered. It is well known that higher-order vortices possess the absolute instability to each kind of distortions [13]. It was shown above that, even for a stable single-sign vortex, the self-restored screened vortex beam is strongly distorted. Therefore, it is clear from the very beginning that a higher-order vortex splits immediately after the screening and will be never restored during the self-treatment. However, which is the space dynamics of its evolution during the diffraction after the screen, and are some singular properties self-restored? To answer these questions, the above-described procedure of computer simulation of the diffraction was used for incident beams with third-order and fifth-order axial vortices.

The evolution of both the phase and OAM distributions for $m = -3$ from the short time $\tau = 0.5$ up to the long time $\tau = 7$ was found (see Fig. 7). We see again the nucleation of two dipoles of diffractive vortices at the short time in the transparent part of the beam (Fig. 7,a).

The first dipole of regenerated vortices appears simultaneously. The band-like $M_z(x, y)$ distribution and the absence of the restoration of a phase spiral reflect the main influence of light diffraction at short times on a higher-order vortex as before on a single-charged vortex. Then, all diffractive vortices annihilate to the long time $\tau = 7$. Three initial-sign subspirals are restored simultaneously. Three initial-sign vortices are concentrated in the central part of the diffracted beam, and the regenerated vortices with opposite sign disappear on the beam periphery (Fig. 7,b). The $M_z(x, y)$ distribution with initial sign occupies the whole right part of the central area of a beam cross-section and a

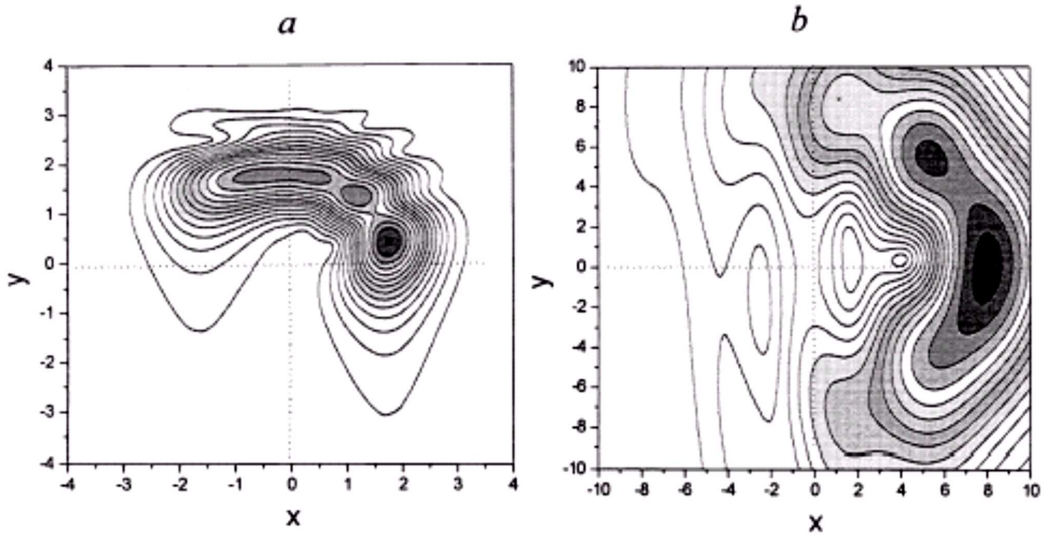

Fig. 6. Amplitude distribution of a diffracted fifth-order axial vortex at $\tau = 0.5$ (a) and $\tau = 5$ (b) for $m = 5$

part of the left half-plane with islands of opposite-sign values of $M_z(x, y)$. The seemed "rotation" of the area with positive value of $M_z(x, y)$ is rather deceptive. We have considered the local intensity as an equivalent of the matter density and have calculated a peculiar beam "mass center". We found that it moves nearly *along* x in the direction of the averaged Poynting vector with nearly constant "speed". The distribution of the total intensity for $\tau = 7$ (Fig. 7,*c*) shows again how strongly it differs from the initial axial symmetric distribution and the location of regenerated vortices nearly along the screen edge. To be sure, we have calculated the diffraction process for $m = -5$. The rotation of the intensity distribution is present again (Fig. 8,*a*,*b*). It was accompanied with the spread of the OAM distribution with initial sign and three connected domains of OAM with opposite sign. Four regenerated single-charge vortices with initial sign are concentrated in the central part. It is seen that the dynamics and the scenario of the self-restoration of a severely screened singular beam is common for axial vortices with arbitrary values of topological charge and is the base to summarize all the obtained results and to make some general conclusions about the main diffraction features of the regeneration of the severely screened vortex beam. They are given below where we will return to a real 3D description of diffraction processes. Only one question remains open: is there a "threshold" value of the screening of a singular beam when singular properties stop to self-treat? The answer to this question is the subject of future investigations.

6. Conclusion: Space Dynamics of the Regeneration of a Screened Vortex Beam

— Diffraction of a severely screened vortex beam differs essentially from that of a light wave with smooth wave front due to the remaining singular properties;

— The vortex beam regeneration process is clearly divided into two groups of events realized at "short" ($z \leq 0.5L_{\mathrm{R}}$) and "long" ($z \geq 1-1.5L_{\mathrm{R}}$) distances behind the obstacle;

— At the beginning, the "diffractive" vortices nucleate in the "transparent" part of the vortex beam at "short" distances due to the interference of the outgoing in-phase and out-of-phase transverse wave systems. They annihilate completely to ($z \geq 1 - 1.5L_{\mathrm{R}}$). The singular properties of the incident beam are still not restored at this stage of the diffracted beam space dynamics.

— The remaining parts of the wave-front helicoid and the orbital angular momentum initiate the process of "self-treatment" of a screened vortex beam at "long" distances behind the screen via the next chain of connected events:

(i) the closed helical wave front is restored, and a new system of the dipoles of secondary vortices nucleates in the beam shadow part. Then the vortices with initial sign concentrate in the central part of the beam cross-section, and the vortices with opposite sign move to the beam periphery and disappear;

(ii) the amplitude distribution "rotates" by $\pi/2$ in the direction opposite to the wave-front helicoid sign according to the Poynting vector orientation;

(iii) the remaining screened beam orbital angular momentum spreads on the beam cross-section and contains domains with initial and opposite signs. The zero-value border $M_z(x, y) = 0$ is the place of location of all secondary vortices.

The self-restored beam loses the axial symmetry and the self-similar propagation, but it possesses main singular properties.

This work was supported by the Science and Technology Center in Ukraine by Partner Project P051.

1. *Born M., Wolf E.* Principles of Optics. — Oxford: Pergamon Press, 1991.
2. *Nye J.F.* // J. Mod. Optics. — 1991. — **38**. — P.743—754.
3. *Basistiy I.V., Soskin M.S., Vasnetsov M.V.* // Opt. Communs.— 1995. — **119**.— P.604—612.
4. *Karman G.-P., Bejersbergen M.W., van Duijil A., Woerdman J.P.*// Opt. Lett.— 1997.— **32**.— P.1503—1505.
5. *Nye J.F.*// J. Opt. Soc. Amer.— 1998.— **A15**.— P.1132—1138.
6. *Berry M.V.* // J. Mod. Optics.— 1998.— **45**.— P.1845—1858.
7. *Sommerfeld A.* // Math. Ann.— 1896.— **47**.— P.317—341.
8. *Khizhnyak A.I., Anokhov S.P., Lymarenko R. et al.* // J. Opt. Soc. Amer. A.— **17** (in press).
9. *Anokhov P., Lymarenko R., Soskin M.S. et al.* // Proc. SPIE "Singular Optics 2000" (in press).
10. *Anokhov S.P., Lymarenko R., Soskin M.S., Khizhnyak A.I.* // Ibid. (in press).
11. *Berry M.V.*// Intern. Conf. on Singular Optics/ Ed. by M.S. Soskin, Proc. of SPIE.— 1998.— **3487**.— P.1—5.
12. *Vasnetsov M.V., Marienko I.G., Soskin M.S.*// Sov. JEPT Lett.— 2000.— **71**, N4.— P.192—196.
13. *Marienko I.G.* Diffraction of Light Beams with Optical Vortices, Ph.D. Thesis, Kyiv, 2000 (in Russian).
14. *Scryabin D.V., Firth W.J.* // Phys. Rev. E.— 1998.— **58**.— P.3916—3930.
15. *Nye J.F., Berry M.V.* // Proc. Roy. Soc. Lond. A.— 1974.— **378**.— P.219—239.
16. *Kreminskaya L.V., Soskin M.S., Khizhnyak A.I.* // Opt. Communs.— 1998.— **145**.— P.377—384.
17. *Allen L., Padgett M.J., Babiker M.* // Progress in Optics/ Ed. by E. Wolf.— 1999.— **39**.— P.291—372.

Received 25.02.05

ДИФРАКЦІЯ СИНГУЛЯРНОГО ПУЧКА НА НЕПРОЗОРОМУ ЕКРАНІ ТА РЕГЕНЕРАЦІЯ ОПТИЧНОГО ВИХОРУ

В.М. Горшков, Г.М. Хорошун, М.С. Соскін

Р е з ю м е

Розвинено теорію дифракції сингулярного світлового пучка на непрозорому екрані з прямолінійним краєм, що перекриває серцевину оптичного вихору. Показано, що дифракція сингулярного пучка значно відрізняється від дифракції світлових пучків з початково гладким хвильовим фронтом. Описано унікальну властивість сингулярного пучка — відновлення гелікоїдальної структури хвильового фронту на певній відстані позаду екрана завдяки впливу довгохвильових поперечних збурень. Цей ефект спостерігається разом зі складною просторовою динамікою утворення та анігіляції вторинних короткоживучих "дифракційних" вихорів. Розглянуто дифракцію одно- та багатозарядового сингулярних пучків. Визначено час та параметри регенерованої структури на основі розвинутої математичної моделі та шляхом аналізу розподілів амплітуди, фази та орбітального кутового момента пучка.